

A dynamic algorithm for palmprint recognition

David Palma

Pier Luca Montessoro

Department of Electrical, Management
and Mechanical Engineering
University of Udine, Italy

Email: palma.david@spes.uniud.it

Email: montessoro@uniud.it

Giulia Giordano

Franco Blanchini

Department of Mathematics
and Computer Science
University of Udine, Italy.

Email: giulia.giordano@uniud.it

Email: franco.blanchini@uniud.it

Abstract—Most of the existing techniques for palmprint recognition are based on metrics that evaluate the distance between a pair of features. These metrics are typically based on static functions. In this paper we propose a new technique for palmprint recognition based on a dynamical system approach, focusing on preliminary experimental results. The essential idea is that the procedure iteratively eliminates points in both images to be compared which do not have enough close neighboring points in the image itself and in the comparison image. As a result of the iteration, in each image the surviving points are those having enough neighboring points in the comparison image. Our preliminary experimental results show that the proposed dynamic algorithm is competitive and slightly outperforms some state-of-the-art methods by achieving a higher genuine acceptance rate.

I. INTRODUCTION

Biometric systems are suitable to be used in various fields, such as high security, forensic and commercial applications. Palmprint recognition, a relatively novel but promising biometric technology, has recently received considerable interest, mostly for its importance in forensics [6] (about 30% of the latents found in crime scenes are from palms [8]) and for several potential civil and security applications [10]. In the literature various palmprint recognition techniques are proposed [15], [20], [21], [22], [24], which can be grouped in two categories: approaches based on low-resolution features and approaches based on high-resolution features, which use creases and ridges, respectively, as local features. The approach discussed in this paper falls under the first category, since it uses as local features the principal lines of the palmprint. Compared with ridges and wrinkles, principal lines are usually the consequence of genetic effects, and therefore are the most significant in palmprint images and have good permanence. However, there may be similar principal lines between different subjects, which makes their distinctiveness relatively low; for this reason, palmprint recognition is a challenging problem.

The proposed system consists of:

- a ROI extraction phase, which follows the typical sequence of steps used in literature [14], [21], to face different issues mainly due to non-linear distortion, such as rotation and translation of the palm with respect to the image, and non-uniform illumination;

- an unconventional feature extraction phase based on the principal lines of the palmprint [24];
- a novel approach to palmprint matching based on a dynamic algorithm. The algorithm involves a positive linear dynamical system [2], whose evolution is determined by the matching level between the two input images: its output converges to zero when the two images have a deep mismatch, while it reaches a high value in the case of good matching.

Exploiting methods based on dynamical systems to improve the performance of an algorithm has led to interesting results in previous work [1].

The rest of paper is as follows: Section II presents the new approach to palmprint recognition based on a noise-rejecting dynamic algorithm; Section III describes the main steps of the preprocessing and feature extraction phases; Section IV reports the preliminary experimental results; Section V gives the conclusion.

II. THE DYNAMIC ALGORITHM FOR PALMPRINT MATCHING

Here we highlight the main idea of the proposed noise-rejecting dynamic (iterative) algorithm for palmprint matching. We consider an operator $(X', Y') = f(X, Y)$ that, given two images $X, Y \in \{0, 1\}^{s \times s}$ (boolean square matrices of size s), provides two new images $X', Y' \in \{0, 1\}^{s \times s}$.

Denoting by $\Sigma(\cdot)$ the number of 1 (active) pixels in an image, the matching index between X and Y is

$$\alpha(X, Y) = \frac{\gamma}{2} \left[\frac{\Sigma(X')}{\Sigma(X)} + \frac{\Sigma(Y')}{\Sigma(Y)} \right], \quad (1)$$

where the coefficient γ is lower when the difference of active pixels in the input images is higher.

The operator f is chosen so as to set to 0 all the pixels without a sufficient number of neighboring 1 pixels, both in the image itself and in the comparison image: only significant clusters of pixels that have a corresponding cluster in the complementary image will remain active.

Given the set \mathcal{N}_{ij} of neighboring points of (i, j) within an integer “radius” $\nu > 0$, the “fading factor” $0 < \lambda < 1$, the coefficient $\mu > 0$ that emphasizes the presence of neighbors in

the comparison image and the tolerance $\epsilon > 0$, the algorithm works as follows.

- The input images are converted from boolean into real arrays $A := X$ and $B := Y$.
- At each iteration: the updated values for each pixel

$$\begin{aligned} x_{ij}(k+1) &= \lambda x_{ij}(k) + \mu \sum_{hl \in \mathcal{N}_{ij}} y_{hl}(k) \\ y_{ij}(k+1) &= \lambda y_{ij}(k) + \mu \sum_{hl \in \mathcal{N}_{ij}} x_{hl}(k) \end{aligned}$$

are computed and then $A := A \times X$, $B := B \times Y$, where \times denotes the componentwise product.

- After all the iterations, the matrices are again converted to boolean: each entry is 0 if below the threshold ϵ , 1 if above. The matching index α is computed as in (1).

So, the value of pixels having no match on the other image will quickly converge to zero; conversely, the value of pixels having a large neighborhood in the comparison image will diverge. In few iterations, some pixels will be practically zero (eventually set to 0), and others will have large values (eventually set to 1). Since all the pixels that are initially 0 remain 0 in view of the componentwise product, $0 \leq \alpha \leq 1$. The correct choice of the parameter values takes place according to the following criterion:

$$\frac{1}{2} < \frac{1 - \lambda}{\mu m} < 1, \quad (2)$$

where m represents the number of pixels in the considered neighborhood. The main advantage of the proposed dynamic approach is its robustness with respect to noise, such as salt and pepper noise: it can be seen that images corrupted with such noise are easily recognized, while an image randomly generated is rejected even if compared with itself [17] since its active pixels are not likely to have enough close neighboring points to survive. In other words, the algorithm intrinsically excludes possible matches between points non belonging to shapes likely related to palm lines.

In order to show an example of how this algorithm works, suppose that the two input images are those shown in figure 1(a) and in figure 1(b), then the result of the dynamic algorithm is shown in figure 1(c).

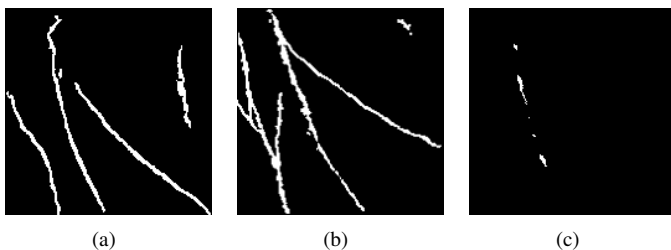


Fig. 1. Dynamic algorithm result: (a), (b) similar principal lines extracted from two different subjects and (c) result of the dynamic algorithm.

As can be seen from the images, the number of survived pixels is very limited, even with similar principal lines. In fact the algorithm has eliminated iteratively points in each image that

do not have enough close neighboring points in the comparison image.

III. PALMPRINT IMAGE PROCESSING

Before the feature extraction phase, a preprocessing phase is essential in order to obtain a sub-image called ROI (Region Of Interest) from the captured palmprint image, which is a 172×172 area of the palmprint's center. In fact, usually palmprint images can have different orientation and size, and are also subject to noise. Moreover, the region of not-interest (e.g., fingers, wrist, image background) may affect the accuracy in verification performance. The preprocessing, aimed to extract and normalize the Region Of Interest (ROI), is a process that will also reduce, to some extent, the effect of rotation and translation of the hand. The main steps of preprocessing are: a preliminary noise reduction and binarization of the hand, then a typical edge detection algorithm such as Canny's operator [3] is applied in order to find the gaps between the fingers. These gaps establish reference points for the computation of the Region Of Interest (ROI) by detecting the boundary of the hand shape and the center from a transformed binary image [21]. Then a normalization is applied in order to have a specific mean and variance for all images [7].

A. Feature extraction

This principal line extraction method, based on [24] and which is illustrated in Figure 2, it does not use a conventional edge detection approach (such as Canny, Sobel, Prewitt, which produce too many trivial lines). The five major steps of this phase are: (i) conversion to a negative image, (ii) lines extraction with Top-Hat filter, (iii) linear contrast adjustment, (iv) binarization with Otsu's method, and (v) noise cleaning with median filter. The details of each step are described below.

1) *Negative*: after normalization in the preprocessing phase, the resultant enhanced ROI image $I(x, y)$ is converted to its negative as follows:

$$I'(x, y) = \max\{I(x, y)\} - I(x, y). \quad (3)$$

2) *Sharpening*: in order to correct uneven illumination a Top-Hat filter is used, then a linear contrast enhancement is applied on the output image. The Top-Hat filtering is defined as the difference between the input image and its morphological opening by a defined structuring element ρ :

$$I'(x, y) = I(x, y) - I(x, y) \circ \rho. \quad (4)$$

This operation returns the bright spots of the image that are smaller than the structuring element.

3) *Contrast adjustment*: a linear contrast enhancement is applied by identifying lower and upper bounds from the histogram, which are the minimum and maximum brightness values in the image, and applying a transformation to stretch this range to fill the full range (0, 255).

4) *Binarization*: a global thresholding is applied at the gray level image resulted from the previous sharpening filter and linear contrast adjustment by using the Otsu's method [16].

5) *Noise cleaning*: here a median filter is used in order to remove noise and trivial lines from the image.

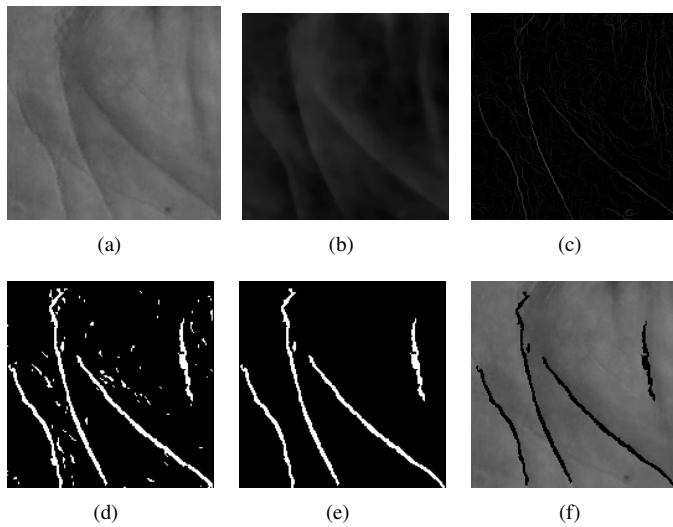


Fig. 2. Feature extraction: (a) original ROI image, (b) after conversion to negative image, (c) after applying sharpening and linear contrast adjustment, (d) after binarization with Otsu's method, (e) after noise cleaning and (f) original palmprint image overlapped with the extracted palm lines.

IV. EXPERIMENTAL RESULTS

In order to evaluate the proposed algorithm, CASIA Palmprint Database [25] has been used as the test dataset. This database contains 5502 palmprint images captured from 312 subjects by a CCD-based device. For each subject, there are palmprint images from both left and right palms and all images are 8 bit gray-level of size 640×480 pixels at 96 dpi resolution. For our tests, we have used right-hand images from 40 subject extracted from the database. The central 172×172 pixels of each hand image, extracted and processed by the feature extraction phase, constitute a template database.

In our experiments, each image in the palmprint database has been matched against the other images. The matching between palmprints which were captured from the same palm is defined as a genuine matching, otherwise as an impostor matching.

The general method to evaluate the performance of a palmprint authentication system is based on the False Acceptance Rate (FAR) and the False Rejection Rate (FRR) [15]. The False Acceptance Rate is defined as the percentage of invalid inputs which are incorrectly accepted and is computed as the number of accepted imposter claims over the total number of imposter accesses. The False Rejection Rate is defined as the percentage of valid inputs which are incorrectly rejected and is computed as the number of rejected genuine claims over the total number of genuine accesses. Other evaluation parameters are:

- Genuine Acceptance Rate: $GAR = 1 - FRR$,
- $GAR_x = GAR|_{FAR=10^{-x}}$ that is the genuine acceptance rate at a specific FAR (e.g. $GAR_2 = GAR|_{FAR=0.01}$),
- Equal Error Rate (EER) that is the error rate at the specific threshold s for which FAR and FRR are equal.

In our tests, we have verified every test pair for each of the palmprint images of the 40 people in the template database. This setup makes for $40 \cdot \binom{8}{2} = 1120$ genuine experiments and $\binom{320}{2} = 51040$ impostor experiments.

EXPERIMENTAL RESULTS

	Parameters	Evaluation set			
		EER	GAR	GAR ₁	GAR ₂
#1	$\lambda = 0.400$ $\mu = 0.035$	0.0505	94.954 %	98.739 %	86.765 %
#2	$\lambda = 0.550$ $\mu = 0.034$	0.0323	96.766 %	98.950 %	92.857 %
#3	$\lambda = 0.500$ $\mu = 0.038$	0.0453	95.475 %	98.529 %	89.916 %
#4	$\lambda = 0.600$ $\mu = 0.030$	0.0609	93.908 %	95.798 %	85.084 %
#5	$\lambda = 0.500$ $\mu = 0.035$	0.0532	94.681 %	96.429 %	89.496 %
#6	$\lambda = 0.560$ $\mu = 0.035$	0.0260	97.398 %	99.790 %	96.429 %

TABLE I

The results of the experiments, expressed in terms of the evaluation parameters above, vary depending on the values of λ and μ in the dynamic algorithm. Table I shows the performance of the proposed algorithm by using different values of the parameters and the marked section would be the best configuration among those we have tested. It is clear that the best configuration, among those we have tested, is actually the sixth, where the equal error rate, i.e., the rate at which FAR and FRR are both minimum, is at 0.026. With this parameter setup, we obtained a GAR₁ value of 99.79%. The corresponding false acceptance rate (FAR) and false rejection rate (FRR) curves at different threshold values are depicted in Figure 4. However, even in the worst case GAR₁ is almost 95.8% whereas the EER is 0.0609. Thus, such a performance is comparable to those of existing palmprint recognition algorithms in the literature [4], [5], [9], [11], [18], [20], [22]. The Receiver Operating Characteristic (ROC) is given by plotting GAR against FAR curve. Figure 3 shows a performance comparison between the best configuration of the proposed approach and two common algorithms, which are Gabor and PCA.

V. CONCLUSION

In this paper, a novel approach has been presented to authenticate individuals by using their palmprint features. As a main contribution, we have proposed a new algorithm that is recursive, hence dynamic. The main advantage of such an approach is its robustness with respect to noise, such as salt and pepper noise: in fact, it can be shown that images corrupted with such a noise are easily recognized, whereas an image randomly generated is rejected even compared with itself [17]. As for the image processing that is necessary for providing the input images to the dynamic algorithm, the first phase involves some preprocessing operations which make the system invariant to rotation and translation of the palm

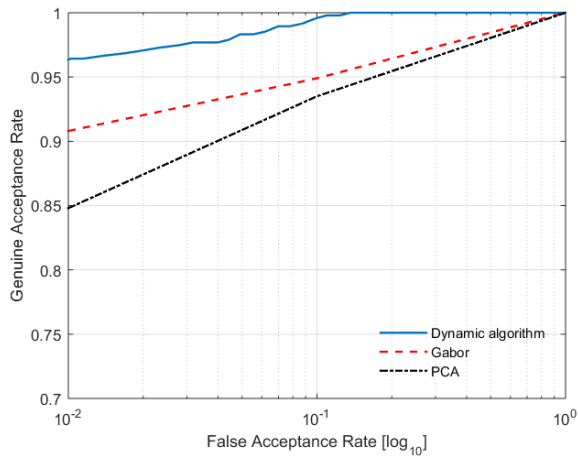


Fig. 3. Comparative Genuine Acceptance Rate against FAR graphs of the dynamic algorithm, Gabor and PCA.

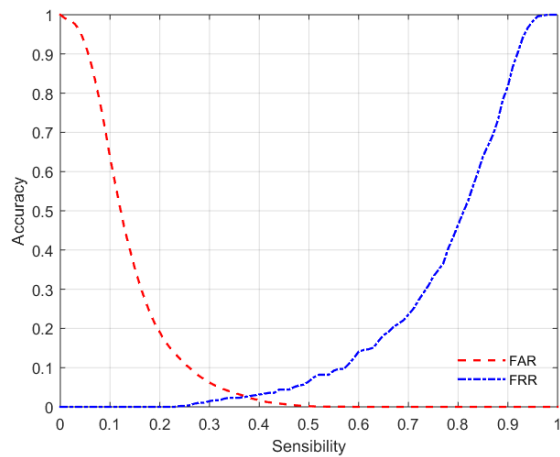


Fig. 4. FAR and FRR curves at different threshold values for configuration number six ($\lambda = 0.56$ and $\mu = 0.035$).

with respect to the image, whereas the second phase consists of a sequence of robust feature extraction steps that allow to detect the principal lines of the palm without introducing noise. Results obtained from the experiments clearly show that the proposed technique is comparable with existing biometric recognition systems based on palmprint recognition and other hand/-based biometric technologies, including hand geometry and fingerprint verification. The experimental results show that the level of GAR₁ can still be considered greater than 98% and the performances of this system are stable when the database size is increased. Moreover, it works quite accurately with low resolution palm images, thus reducing the computational cost.

REFERENCES

- [1] F. Blanchini, D. de Caneva, P.L. Montessoro, and D. Pierattoni, *Control-based p-persistent adaptive communication protocol*, ACM Transactions on Autonomous and Adaptive Systems, vol. 7, no. 2, pp. 29:1–29:18, 2012.
- [2] F. Blanchini and S. Miani, *Set-theoretic methods in control*, ser. Systems & Control: Foundations & Applications. Boston: Birkhäuser, 2008.
- [3] J. Canny, *A computational approach to edge detection*, IEEE Transactions on Pattern Analysis and Machine Intelligence, vol. 8, no. 6, pp. 679–698, 1986.
- [4] T. Connie, A. Teoh, M. Goh and D. Ngo, *Palmprint recognition with PCA and ICA*, Proc. Image and Vision Computing, New Zealand. 2003.
- [5] T. Connie, A.T.B. Jin, M.G.K.Ong, and D.N.C. Ling, *An automated palmprint recognition system*, Image and Vision computing, vol. 23, no. 5, pp. 501–515, 2005. ISO 690
- [6] R. Cappelli, M. Ferrara and D. Maio, *A Fast and Accurate Palmprint Recognition System Based on Minutiae*, IEEE Transactions on Systems, Man and Cybernetics, vol. 42, no. 3, pp. 956–962, 2012.
- [7] L. Hong, Y. Wan, and A. Jain, *Fingerprint image enhancement: Algorithm and performance evaluation*, IEEE Transactions on Pattern Analysis and Machine Intelligence, vol. 20, no. 8, pp. 777–789, 1998.
- [8] A.K. Jain and J. Feng, *Latent palmprint matching*, IEEE Transactions on Pattern Analysis and Machine Intelligence, vol. 31, no. 6, pp. 1032–1047, 2009.
- [9] A.K. Jain, S. Prabhakar, L. Hong and S. Pankanti, *Filterbank-based fingerprint matching*, IEEE Transactions on Image Processing, vol. 9, no. 5, pp. 846–859, 2000.
- [10] A. Kong, D. Zhang and M. Kamel, *A survey of palmprint recognition*, Pattern Recognition, vol. 42, no. 7, pp. 1408–1418, 2009.
- [11] A.W.K. Kong, D. Zhang and W. Li, *Palmprint feature extraction using 2-D Gabor filters*, Pattern Recognition, vol. 36, no. 10, pp. 2339–2347, 2003.
- [12] K. Krishneswari and S. Arumugam, *Intramodal feature fusion based on PSO for palmprint authentication*, ICTACT Journal on Image and Video Processing, vol. 2, no. 4, pp. 435–440, 2012.
- [13] A. Kumar, M. Wong, H.C. Shen, and A.K. Jain, *Personal verification using palmprint and hand geometry biometric*, Proceedings of the 4th international conference on Audio- and video-based biometric person authentication, pp. 668–678, 2003.
- [14] M.A. Leo Vijilious and V. Subbiah Bharathi, *Texture feature extraction approach to palmprint using nonsubsampling contourlet transform and orthogonal moments*, International Journal of Future Computer and Communication, vol. 1, no. 3, pp. 298–301, 2012.
- [15] J.S. Noh and K.H. Rhee, *Palmprint identification algorithm using Hu invariant moments and Otsu binarization*, in Proceedings of the Fourth Annual ACIS International Conference on Computer and Information Science, pp. 94–99, 2005.
- [16] N. Otsu, *A threshold selection method from gray-level histograms*, IEEE Transactions on Systems, Man and Cybernetics, vol. 9, no. 1, pp. 62–66, 1979.
- [17] D. Palma, P.L. Montessoro, G. Giordano and F. Blanchini, *Palmprint recognition: a dynamical system approach*, in preparation.
- [18] R. Sanchez-Reillo, C. Sanchez-Avilla, and A. Gonzalez-Marcos, *Biometric identification through hand geometry measurements*, IEEE Transactions on Pattern Analysis and Machine Intelligence, vol. 22, no. 10, pp. 1168–1171, 2000.
- [19] X. Wu, K. Wang, D. Zhang, *Palm line extraction and matching for personal authentication*, IEEE Transactions on Systems, Man and Cybernetics, vol. 36, no. 5, pp. 978–987, 2006b.
- [20] J. You, W. Li and D. Zhang, *Hierarchical palmprint identification via multiple feature extraction*, Pattern Recognition, vol. 35, no. 4, pp. 847–859, 2002.
- [21] D. Zhang, W.K. Kong, J. You and M. Wong, *Online palmprint identification*, IEEE Transactions on Pattern Analysis and Machine Intelligence, vol. 25, no. 9, pp. 1041–1050, 2003.
- [22] B. Zhang, W. Li, P. Qing and D. Zhang, *Palm-print classification by global features*, IEEE Transactions on Systems, Man and Cybernetics, vol. 43, no. 2, pp. 370–378, 2003.
- [23] D. Zhang, W. Shu, *Two novel characteristics in palmprint verification: datum point invariance and line feature matching*, Pattern Recognition, vol. 32, no. 4, pp. 691–702, 1999.
- [24] Z.J. Zia-uddin, Z. Jan, J. Ahmad and A. Abbasi, *A novel technique for principal lines extraction in palmprint using morphological Top-Hat filtering*, World Applied Sciences Journal, vol. 31, no. 12, pp. 2010–2014, 2014.
- [25] Chinese Academy of Sciences Institute of Automation, *CASIA Palmprint Image Database*, available at the url: “<http://biometrics.idealtest.org/>”.